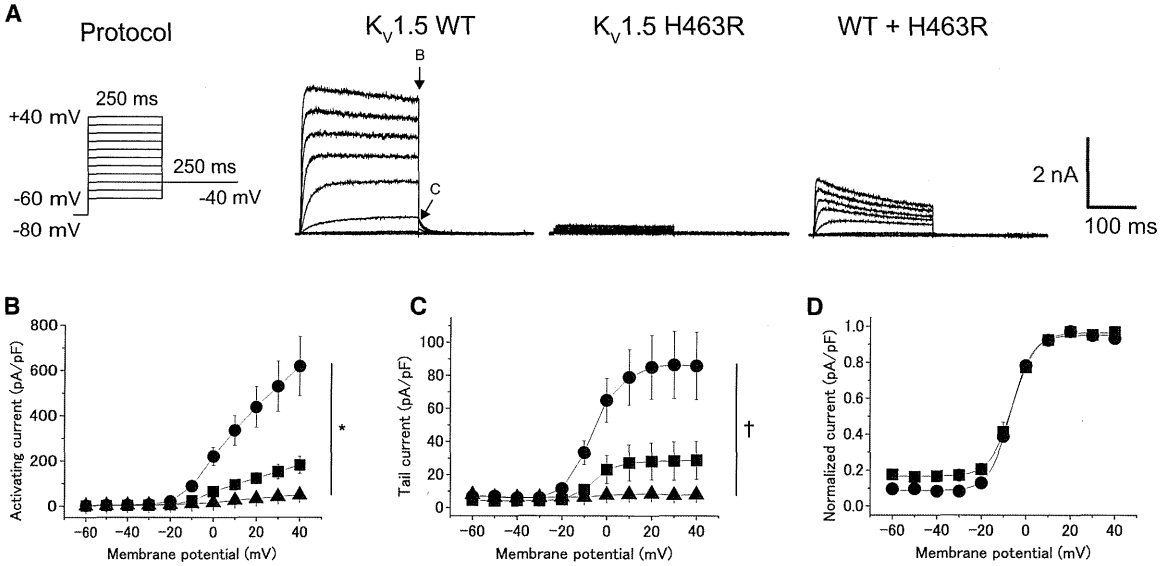

Figure 2. Functional characterization of K_V1.5 H463R in HEK293 cells. **A**, Representative currents generated in HEK293 cells that had been transfected with 0.2 μg of a vector expressing wild-type (WT) *KCNA5* alone (**left**), 0.2 μg of a vector expressing *KCNA5* H463R alone (**middle**), or 0.1 μg of each of the *KCNA5* WT and *KCNA5* H463R vectors (**right**). Pulse protocol is shown in the inset. **B** and **C**, *I–V* relationships for peak currents (**B**) and tail currents (**C**) in HEK293 cells expressing WT alone (closed circle, n=20), H463R (closed triangle, n=9), and WT+H463R (closed square, n=15). **D**, Mean amplitudes of normalized tail currents for WT alone (closed circle, n=17) and WT+H463R (closed square, n=8). **P*<0.001 or †*P*<0.01 among indicated current–voltage relationships by 2-way repeated-measures ANOVA.

Whole-cell patch clamp experiments were conducted on CHO-K1 cells transfected with vectors expressing K_V7.1 WT or K_V7.1 L492_E493insDL. The activating and tail current amplitudes of K_V7.1 WT/KCNE1 were similar to those of the K_V7.1 mutant/KCNE1 (Figure IA–IC and Table I in the Data Supplement; Table 4). The normalized tail current–voltage relationship for K_V7.1 WT/KCNE1 channels was also similar to that for K_V7.1 mutant/KCNE1 channels (Figure ID and Table I in the Data Supplement).

Clinical Characteristics and Functional Properties of *KCNH2* Variants

The proband who was heterozygous for *KCNH2* T436M was a 61-year-old man with onset of AF at the age of 38. The ECG showed chronic AF and a normal QTc interval (Table 3). His brother and sister had been affected with AF from a young age.

Table 4. In Vitro Cellular Electrophysiology

Gene	Amino Acid Change	Current Density	Channel Kinetics
KCNA5	H463R	Absent I_{Kur}	No change
	T527M	Increased peak and tail currents	Faster activation
KCNQ1	L492_E493 ins DL	No change	No change
KCNH2	T436M	Increased peak currents	Slower deactivation
	T895M	Increased peak and tail currents	Slower deactivation
SCN5A	R986Q	Decreased peak currents	No change
SCN1B	T189M	Increased peak currents	Negative shift in steady-state activation

We transiently expressed WT and T436M in cultured mammalian CHO-K1 cells for whole-cell voltage clamp measurements (Figure II in the Data Supplement; Table 4). Electrophysiological studies showed that the peak current density for T436M was significantly greater than that for the WT (Figure IIB and Table II in the Data Supplement). No significant difference in activation kinetics or the steady-state inactivation kinetics was observed between the mutant and WT channels (Figure IID and IIF and Table II in the Data Supplement). In contrast, slow and fast time constants in the mutant channel were increased significantly compared with those of the WT (Figure IIE and Table II in the Data Supplement). Two-way repeated-measures ANOVA revealed that the fast time constants were significantly increased in the T436M compared with the WT (Figure IIE in the Data Supplement). In silico prediction analysis indicated that T436M was potentially benign, according to 5 algorithms (Table 5).

The proband who was heterozygous for *KCNH2* T895M was a 58-year-old man with onset of AF at the age of 40 (Table 3). The ECG showed a normal QTc interval. He underwent radiofrequency catheter ablation at the age of 59. His father, who also carried T895M in *KCNH2*, had experienced paroxysmal palpitations since his early 50s and developed a transient ischemic attack at the age of 81. The proband's son, who carried the same variant, had also experienced paroxysmal palpitations about once a week since his late 20s.

When we transiently expressed WT and T895M in cultured mammalian CHO-K1 cells for whole-cell voltage clamp

Table 5. In Silico Prediction Analysis

Gene	Amino Acid Change	Polyphen-2	Grantham	SIFT Score	PROVEAN Score	Score CADD
KCNA5	H463R	0.195	29	0.031, damaging	−3.49, deleterious	14.25, deleterious
	T527M	0.954, possibly damaging	81	0.007, damaging	−4.96, deleterious	19.35, deleterious
KCNQ1	L492_E493 ins DL	N/A	N/A	N/A	N/A	N/A
KCNH2	T436M	N/A	78	0.138	−0.42	1.52
	T895M	N/A	78	0.178	−1.57	17.78, deleterious
SCN5A	R986Q	N/A	103, radical	0.308	−0.62	11.17, deleterious
SCN1B	T189M	N/A	113, radical	0, damaging	−0.08	15.27, deleterious

CADD indicates Combined Annotation Dependent Depletion; N/A, not available; PROVEAN, Protein Variation Effect Analyzer; and SIFT, Sorting Intolerant From Tolerant.

measurements, we observed a larger current for the mutant channel than the WT channel (Figure 4). Electrophysiological studies showed that the peak and tail current densities for T895M were significantly larger than those for the WT, respectively (Figure 4B and 4C; Table II in the Data Supplement; Table 4). No significant difference in activation kinetics or the steady-state inactivation kinetics when compared with the WT was observed (Figure 4D and 4F; Table II in the Data Supplement). In contrast, both slow and fast deactivation time constants for the mutant channel were increased significantly compared with those of the WT for voltages at −40 and −30 mV (Figure 4E; Table II in the Data Supplement). In silico analysis predicted that T895M was likely to be pathogenic, although only according to the score CADD (Table 5).

Clinical Characteristics and Functional Properties of *SCN5A* and *SCN1B* Variants

The proband who was heterozygous for *SCN5A* R986Q was a 64-year-old man with onset of paroxysmal AF at the age of 58 (Table 3). None of his family members had clinical signs of AF.

CHO-K1 cells were transiently transfected with vectors expressing WT or R986Q cDNA and the human β1 subunit cDNA in combination with a bicistronic plasmid encoding green fluorescent protein. Compared with the WT, R986Q significantly reduced the peak sodium current density (; Table 4 Figure IIIB and Table III in the Data Supplement). No significant difference was observed in the voltage-dependence of steady-state activation or the voltage-dependence of steady-state fast inactivation (Figure IIIC and IIID and Table III in the Data Supplement). In silico analysis predicted that R986Q was pathogenic, according to 2 algorithms (Table 5).

SCN1B T189M was detected in 2 probands with lone AF (Table 3). One proband who was homozygous for the variant was a 59-year-old woman who showed paroxysmal AF with palpitations every few months. Her AF was always terminated soon after taking pilsicainide. Her daughter, who was heterozygous for the variant, was a 33-year-old woman and had never experienced paroxysmal palpitations. The second proband, who

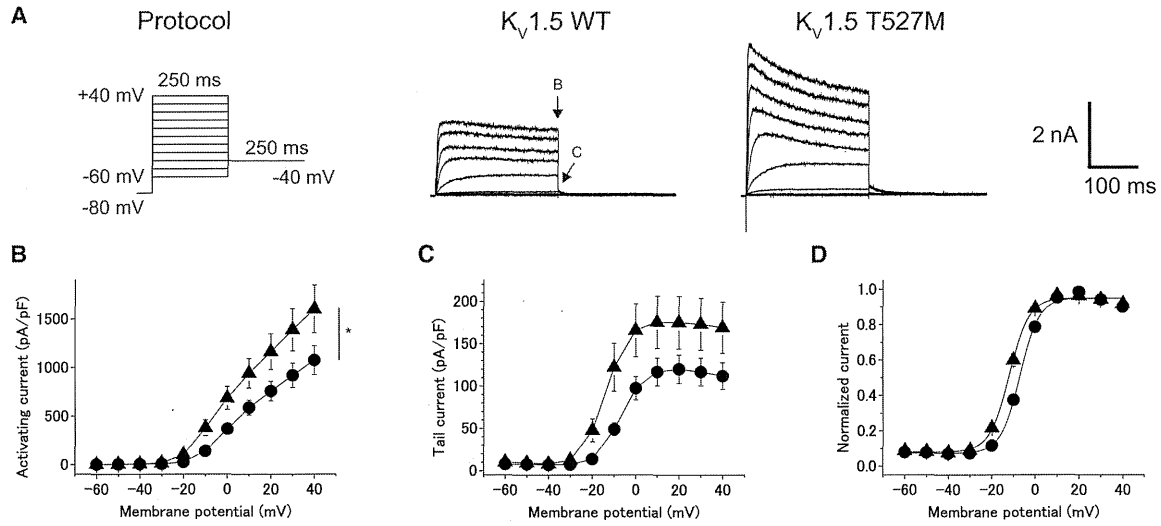

Figure 3. Functional characterization of K_V1.5 T527M in HEK293 cells. **A**, Representative currents generated in HEK293 cells, transfected with 0.2 μg of a vector expressing *KCNA5* WT alone (**left**) or 0.2 μg of a vector expressing *KCNA5* T527M alone (**right**). **B** and **C**, *I–V* relationships for peak currents (**B**) and tail currents (**C**) in HEK293 cells transfected with the wild-type (WT) vector alone (closed circle, n=33) or the T527M vector (closed triangle, n=47). **D**, Mean amplitudes of normalized tail currents for WT alone (closed circle, n=33) and T527M alone (closed triangle, n=42). *P<0.05 between the indicated current–voltage relationships by 2-way repeated-measures ANOVA.

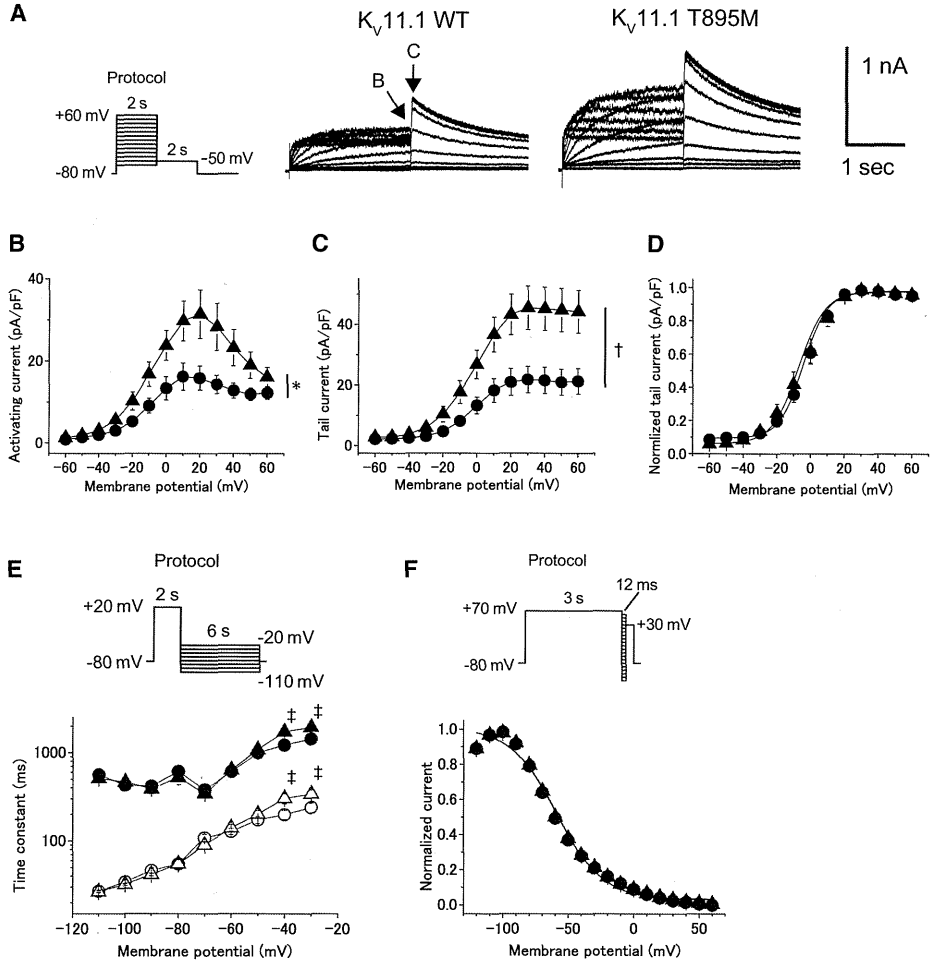

Figure 4. Functional characterization of K_V11.1 T895M in CHO-K1 cells. **A**, Representative currents generated in CHO-K1 cells, transfected with 1 μg of a vector expressing *KCNH2* wild-type (WT) alone (**left**) or 1 μg of a vector expressing *KCNH2* T895M alone (**right**). Pulse protocol is shown in the inset. **B** and **C**, *I–V* relationships for peak currents (**B**) and tail currents (**C**) in CHO-K1 cells transfected with WT alone (closed circle, n=18) and T895M (closed triangle, n=18). **D**, Mean amplitudes of normalized tail currents for WT alone (closed circle, n=10) and T895M (closed triangle, n=13). **E**, Deactivation time constants of K_V11.1 currents (protocol shown in the inset). The deactivation process was fitted to biexponential functions. Deactivation time constants of WT (fast component: open circle, n=13; slow component: closed circle, n=13) and T895M (fast component: open triangle, n=15; slow component: closed triangle, n=15) are shown. **F**, Normalized steady-state inactivation curves for WT (closed circle, n=9) and T895M (closed triangle, n=11). Pulse protocol is shown in the inset. The current amplitude at the test potential was normalized and plotted against the prepulse potential. Curves represent the best fits to a Boltzmann function. **P*<0.01 or †*P*<0.05 between the indicated current–voltage relationships by 2-way repeated-measures ANOVA. ‡*P*<0.05 vs WT by Student *t* test.

was heterozygous for the variant, was a 55-year-old woman who showed paroxysmal AF that was controlled well by pilsicainide. This variant was also detected in a control subject in his 20s.

Threonine at 189 is located in the C terminus of the $Na_V\beta1$ subunit and is highly conserved among the mammalian homologs of this protein. Thus, we performed electrophysiological analysis of the mutant $Na_V\beta1$ protein. When we coexpressed $Na_V1.5$ with the mutant $Na_V\beta1$ subunit, the expressed current density was significantly larger than that observed with the WT $Na_V\beta1$ subunit (Figure 5A; Table 4). The maximum peak current density of $Na_V1.5$ plus $Na_V\beta1$ T189M, measured at −30 mV, was −463±100 pA/pF, which was significantly smaller than the −240±34 pA/pF for $Na_V1.5$ plus $Na_V\beta1$ WT (Figure 5B; Table III in the Data Supplement). *I–V* curves of normalized peak sodium current showed that the mutant channel resulted in a significant negative voltage shift of steady-state activation when compared with the WT channel (Figure 5C; Table III in the Data Supplement). No significant difference was observed in the voltage dependence of steady-state fast inactivation (Figure 5D; Table III in the Data Supplement). In silico analysis predicted that T189M was pathogenic, according to 3 algorithms (Table 5).

In Silico Prediction Analysis of Rare Variants Associated With Lone AF

CADD is an integrated algorithm based on a total of 65 annotations; this approach predicted that both *KCNA5* variants (H463R and T527M), *KCNH2* T895M, *SCN5A* R986Q,

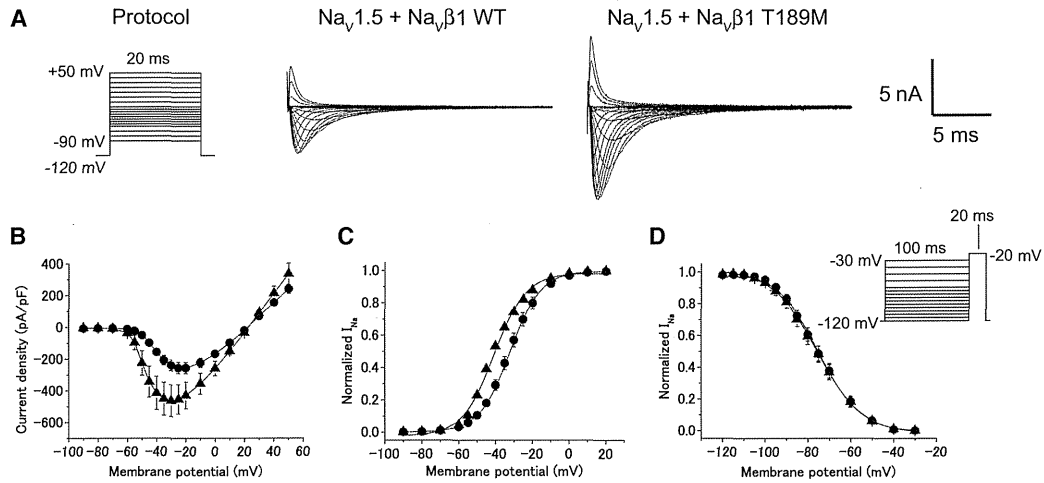

Figure 5. Functional characterization of Na$_V$1.5+Na$_V$β1 T189M in CHO-K1 cells. **A**, Representative currents generated in CHO-K1 cells that had been transfected with 0.6 μg each of a vector expressing the Na$_V$1.5 channel and wild-type (WT) Na$_V$β1 subunit (**left**) or 0.6 μg each of a vector expressing the Na$_V$1.5 channel and mutant Na$_V$β1 subunit (**right**). Pulse protocol is shown in the inset. **B**, *I–V* relationships for peak currents of Na$_V$1.5+Na$_V$β1 WT (closed circle, n=16) or Na$_V$1.5+Na$_V$β1 mutant (closed triangle, n=16). **C** and **D**, Voltage dependence of the steady-state activation and fast inactivation of Na V1.5+Na$_V$β1 WT (closed circle, n=16) or Na$_V$1.5+Na$_V$β1 mutant (closed triangle, n=16), measured using standard pulse protocols.

and *SCN1B* T189M were deleterious (CADD score, >10; Table 5). Seven variants were divided into 3 categories on the basis of their cellular electrophysiological profile and CADD scores: (1) cellular electrophysiologically abnormal and bioinformatically deleterious variants, including *KCNA5* H463R and T527M, *KCNH2* T895M, *SCN5A* R986Q, and *SCN1B* T189M; (2) cellular electrophysiologically abnormal and bioinformatically benign variant, including *KCNH2* T436M; and (3) cellular electrophysiologically normal but bioinformatically radical variant, including *KCNQ1* L492_E493 ins DL (Figure 6).

We also investigated how many rare (MAF, <1%) variants were predicted to be deleterious using an in silico prediction tool (CADD scores, >10) and how many such alleles were present in the 12 AF-associated genes, in the largest exome sequencing study to date, using 61 486 unrelated individuals (ExAC data and browser).[12] We found as many as 2255 variants (17 859 alleles) that could potentially be (mis)judged as causative based only on these frequency/in silico prediction tool strategies (Figure IV in the Data Supplement).

Discussion

In this study, we analyzed 90 patients with lone AF for rare genetic variants in 12 genes and identified 7 rare variants in 8 patients. This indicates that 8.9% of patients with lone AF carry rare genetic variants. Of these 7 variants, 2 variants were identified in the 250 control subjects (MAF, 0.2% each), 1 variant was reported in the EVS (MAF, <0.01%), and 3 variants were reported in the ExAC (MAF, <0.05% each). More variants were reported in the ExAC than the EVS, likely because the ExAC includes data of east and south Asia, whereas the EVS comprises data of black and European American individuals. Because the MAFs of 3 variants (*KCNA5* T527M, *KCNH2* T436M, and *SCN5A* R986Q) in the ExAC database were significantly smaller than those in our case population, these seem to be extremely rare variants. Recently, Olesen et al[17] reported that 29 rare variants had been identified among 192 patients with early-onset lone AF (onset of disease before the age of 40). The frequency of rare variants in our lone AF cohort (8.9%) was lower than that in Olesen's study (15.1%). There are several reasons for the difference in frequency: (1) our cohort included individuals with onset of lone AF at an

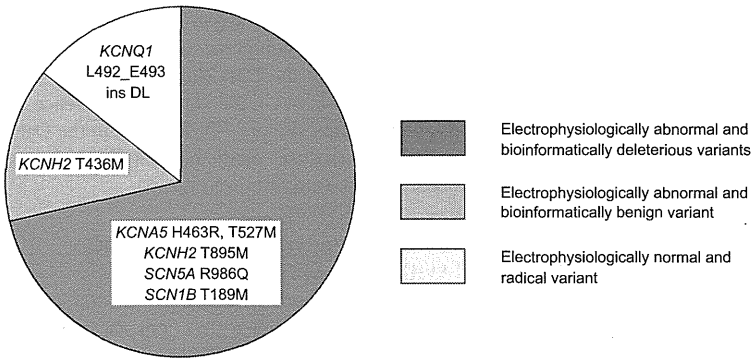

Figure 6. Classification of rare variants according to their electrophysiological and bioinformatic properties. Seven rare variants detected in this study were divided into 3 groups: cellular electrophysiologically abnormal and bioinformatically deleterious variants, cellular electrophysiologically abnormal and bioinformatically benign variants, and cellular electrophysiologically normal and bioinformatically radical variants.

older age, (2) Olesen et al[17] defined rare variants as variants with an MAF of <0.1% in the EVS, and (3) they performed screening of genomic DNA for 14 genes, whereas 12 genes were investigated in our study.

More than 100 rare variants have been reported in patients with lone AF[7–9]; however, the functional effect of most variants has not been evaluated. In this study, we carefully characterized each of the rare variants and could find that they have novel or overt abnormalities in channel function.

One of the 2 *KCNA5* variants identified in this study, H463R, was a novel mutation; the histidine at codon 463 is located in the S5-pore loop, in the vicinity of the pore of the $K_V1.5$ subunit. Our patch clamp study showed that this mutation caused dominant-negative suppression of $K_V1.5$ WT function and was considered to have a loss-of-function effect. The loss-of-function mutation in the *KCNA5* gene can lead to a decrease in I_{Kur}, action potential prolongation, and early after-depolarization. The other *KCNA5* variant, T527M, showed a gain-of-function effect with an enhanced steady-state activation, which was revealed by electrophysiological analysis. A previous study reported that 3 gain-of-function variants in *KCNA5* displayed a negative voltage shift in the steady-state activation curves.[18] The T527 variant had previously been identified in a Chinese family with AF.[19]

We identified 2 *KCNH2* variants with gain-of-function effects in patients with lone AF, although only a few *KCNH2* variants have so far been reported in patients with lone AF.[20] *KCNH2* T436M had previously been identified in a long QT syndrome family with low disease penetrance.[21] The proband in our study was affected with AF from the age of 38 and had a number of AF-affected family members. Furthermore, *KCNH2* T895M had previously been identified in a patient with sudden infant death syndrome.[22] In our study, the proband's father and son, who both carried the T895M variant, had paroxysmal palpitations. Our cellular electrophysiological studies showed that the deactivation time course in both these $K_V11.1$ channels were significantly slower than that in the WT channel, which resulted in a gain-of-function effect. A previous study of T895M in *Xenopus* oocytes showed that the deactivation time constants in the T895M channel were increased significantly compared with those of the WT,[22] which corresponded to our results. The gain-of-function *KCNH2* variants implicated in susceptibility to AF may exist more frequently than indicated in previous reports.

Several *KCNQ1* gain-of-function mutations have been identified in patients with lone AF to date.[8] We found a *KCNQ1* insertion variant (L492_E493insDL) in a lone AF proband with normal QTc intervals. This is a so-called radical variant, which is likely to be pathogenic; however, its channel properties were similar to those of the WT channel.

We found a rare *SCN5A* variant, R986Q, in patients with lone AF. In a heterologous expression study, R986Q was categorized as a loss-of-function variant and can cause shortening of the refractory period and slowing of conduction. We also identified an *SCN1B* T189M variant in 2 probands with lone AF and in 1 of 250 control subjects in this study. Previously, several *SCN1B* variants have been reported in patients with AF and had a loss-of-function effect.[8,23] Our cellular electrophysiological study showed that T189M was a gain-of-function variant, which was predicted to lower the threshold potential for cellular excitability. This is the first report on an AF-associated *SCN1B* variant that leads to an increased peak sodium current density and that changes the voltage dependence of the steady-state fast activation of the Na^+ channel. Moreover, our data indicated that the sodium-channel blocker pilsicainide was effective for AF in probands with gain-of-function variants in *SCN1B*.

Many prediction tools are available for predicting a pathogenic or benign status for rare variants identified in patients with various genetic disorders.[14,24,25] Giudicessi et al[14] tested whether 4 prediction tools—conservation analysis, Grantham values, Sorting Intolerant From Tolerant, and PolyPhen2—have the potential to enhance the classification of rare nonsynonymous single-nucleotide variants in type 1 and 2 long QT syndromes. Their findings supported the potential synergistic utility of these tools to enhance the classification of rare variants; however, their use in isolation in clinical application remains limited. CADD is an attractive prediction tool that uses a total of 65 annotations, including gene models, conservation measures, and ENCODE data summaries.[16] In this study, 5 of 6 variants exhibiting electrophysiological abnormalities were predicted to be pathogenic according to their CADD scores, reinforcing classification of these rare variants as pathogenic in patients with lone AF.

Several clinical applications can be derived from this study. First, at least 9% of patients with lone AF have a rare variant in cardiac ion-channel genes. Four of 7 rare variants implicated in susceptibility to AF showed gain-of-function effects by electrophysiological studies. Second, rare ion-channel variants identified in patients with lone AF have therapeutic implications.[10] In particular, patients with gain-of-function variants are likely to benefit from a drug that enables selective inhibition of mutant channel complexes. A previous study showed the enhanced sensitivity of *KCNQ1* gain-of-function mutations for the I_{Ks} selective blocker HMR-1556.[26] In our study, sodium-channel blockers were shown to be effective in patients harboring *SCN1B* T189M. Similarly, I_{Kur} channel blocking or I_{Kr} channel blocking may be effective for preventing the shortening of action potential duration in patients with *KCNA5* T527M or *KCNH2* T436M and T895M. Thus, genetic testing of major ion-channel genes for patients with lone AF is therefore significant. In addition, the rare variants annotated as pathogenic by CADD should be evaluated to determine whether they have loss-of-function or gain-of-function effects by electrophysiological studies. Third, several asymptomatic family members with rare variants were identified in this study and may have a risk of developing AF in future. These subjects should be advised to avoid acquired risk factors for the development of AF, and preventive care for reducing these risk factors should be provided.

Study Limitations

This study has several limitations. First, 12 major genes were examined here for rare variants associated with AF and were only a small fraction of potential genes related to AF. Whole-exome sequencing or targeted next-generation sequencing may reveal more variants associated with AF in many genes. Second, the case population (n=90) and the control population (n=250) used in this study were relatively small. Indeed,

recent reports studied 192 to 307 patients with lone AF or 216 to 240 healthy subjects as a reference.[18,27] However, we used data from the EVS[11] and the ExAC data and browser[12] as reference groups. Finally, only the individual variants identified in the cases were evaluated in the control population. It is possible that a series of rare variants may have been identified in the controls if the rest of the coding region of each gene had been fully screened in the controls. In fact, 2255 rare and deleterious variants (MAF, <1%; CADD scores, >10) in 12 AF-associated genes were found in the ExAC data and browser,[12] which comprises in excess of 60000 unrelated individuals sequenced (Figure IV in the Data Supplement). This emphasizes the importance of both phenotype assessments and functional analyses for the determination of disease-causing variants even in this comprehensive genotyping era.

Conclusions

In our cohort of patients with lone AF, 7 rare variants in cardiac ion-channel genes were identified in 8 probands, with a prevalence of ≈9%. These variants were extremely rare and characterized as causing susceptibility to AF by either electrophysiological study or in silico prediction analysis. More than half of AF-associated rare variants showed gain-of-function behavior, which is likely to benefit from a drug that blocks particular ion channels.

Acknowledgments

We gratefully acknowledge Drs Higashida, Yokoyama, Tanii, and Oka for statistical advice and helpful discussions; Drs Tsuchiya and Oe for providing patient's phenotype data; and T. Obayashi, M. Fukagawa, H. Oikawa, and S. Nakano for technical assistance.

Sources of Funding

This study was supported by grants from Grant-in Aid for Scientific Research from the Japan Society for the Promotion of Science (19790520 to K.Hayashi), the Ministry of Health, Labor, and Welfare of Japan for Clinical Research on Intractable Diseases (H26-040 and H24-033 to K. Hayashi), and Takeda Science Foundation (K. Hayashi).

Disclosures

None.

References

1. Andrade J, Khairy P, Dobrev D, Nattel S. The clinical profile and pathophysiology of atrial fibrillation: relationships among clinical features, epidemiology, and mechanisms. *Circ Res.* 2014;114:1453–1468. doi: 10.1161/CIRCRESAHA.114.303211.
2. Brand FN, Abbott RD, Kannel WB, Wolf PA. Characteristics and prognosis of lone atrial fibrillation. 30-year follow-up in the Framingham Study. *JAMA.* 1985;254:3449–3453.
3. Darbar D, Herron KJ, Ballew JD, Jahangir A, Gersh BJ, Shen WK, Hammill SC, Packer DL, Olson TM. Familial atrial fibrillation is a genetically heterogeneous disorder. *J Am Coll Cardiol.* 2003;41:2185–2192.
4. Oyen N, Ranthe MF, Carstensen L, Boyd HA, Olesen MS, Olesen SP, Wohlfahrt J, Melbye M. Familial aggregation of lone atrial fibrillation in young persons. *J Am Coll Cardiol.* 2012;60:917–921. doi: 10.1016/j.jacc.2012.03.046.
5. Everett BM, Cook NR, Conen D, Chasman DI, Ridker PM, Albert CM. Novel genetic markers improve measures of atrial fibrillation risk prediction. *Eur Heart J.* 2013;34:2243–2251. doi: 10.1093/eurheartj/eht033.
6. Tada H, Shiffman D, Smith JG, Sjogren M, Lubitz SA, Ellinor PT, Louie JZ, Catanese JJ, Engstrom G, Devlin JJ, Kathiresan S, Melander O. Twelve-single nucleotide polymorphism genetic risk score identifies individuals at increased risk for future atrial fibrillation and stroke. *Stroke.* 2014;45:2856–2862. doi: 10.1161/STROKEAHA.114.006072.
7. Chen YH, Xu SJ, Bendahhou S, Wang XL, Wang Y, Xu WY, Jin HW, Sun H, Su XY, Zhuang QN, Yang YQ, Li YB, Liu Y, Xu HJ, Li XF, Ma N, Mou CP, Chen Z, Barhanin J, Huang W. KCNQ1 gain-of-function mutation in familial atrial fibrillation. *Science.* 2003;299:251–254.
8. Olesen MS, Nielsen MW, Haunso S, Svendsen JH. Atrial fibrillation: the role of common and rare genetic variants. *Eur J Hum Genet.* 2014;22:297–306. doi: 10.1038/ejhg.2013.139.
9. Tucker NR, Ellinor PT. Emerging directions in the genetics of atrial fibrillation. *Circ Res.* 2014;114:1469–1482. doi: 10.1161/CIRCRESAHA.114.302225.
10. Darbar D, Roden DM. Genetic mechanisms of atrial fibrillation: impact on response to treatment. *Nat Rev Cardiol.* 2013;10:317–329. doi: 10.1038/nrcardio.2013.53.
11. NHLBI Exome Sequencing Project (ESP). Exome Variant Server Web site. http://evs.gs.washington.edu/EVS/. Accessed January 02, 2015.
12. ExAC Browser (Beta)|Exome Aggregation Consortium Website. http://exac.broadinstitute.org/. Accessed January 02, 2015.
13. Hayashi K, Fujino N, Uchiyama K, Ino H, Sakata K, Konno T, Masuta E, Funada A, Sakamoto Y, Tsubokawa T, Nakashima K, Liu L, Higashida H, Hiramaru Y, Shimizu M, Yamagishi M. Long QT syndrome and associated gene mutation carriers in Japanese children: results from ECG screening examinations. *Clin Sci (Lond).* 2009;117:415–424. doi: 10.1042/CS20080528.
14. Giudicessi JR, Kapplinger JD, Tester DJ, Alders M, Salisbury BA, Wilde AA, Ackerman MJ. Phylogenetic and physicochemical analyses enhance the classification of rare nonsynonymous single nucleotide variants in type 1 and 2 long-QT syndrome. *Circ Cardiovasc Genet.* 2012;5:519–528. doi: 10.1161/CIRCGENETICS.112.963785.
15. Choi Y, Sims GE, Murphy S, Miller JR, Chan AP. Predicting the functional effect of amino acid substitutions and indels. *PLoS One.* 2012;7:e46688. doi: 10.1371/journal.pone.0046688.
16. Kircher M, Witten DM, Jain P, O'Roak BJ, Cooper GM, Shendure J. A general framework for estimating the relative pathogenicity of human genetic variants. *Nat Genet.* 2014;46:310–315. doi: 10.1038/ng.2892.
17. Olesen MS, Andreasen L, Jabbari J, Refsgaard L, Haunso S, Olesen SP, Nielsen JB, Schmitt N, Svendsen JH. Very early-onset lone atrial fibrillation patients have a high prevalence of rare variants in genes previously associated with atrial fibrillation. *Heart Rhythm.* 2014;11:246–251. doi: 10.1016/j.hrthm.2013.10.034.
18. Christophersen IE, Olesen MS, Liang B, Andersen MN,Larsen AP, Nielsen JB, Haunso S, Olesen SP, Tveit A, Svendsen JH, Schmitt N. Genetic variation in KCNA5: impact on the atrial-specific potassium current IKur in patients with lone atrial fibrillation. *Eur Heart J.* 2013;34:1517–1525. doi: 10.1093/eurheartj/ehs442.
19. Yang Y, Li J, Lin X, Yang Y, Hong K, Wang L, Liu J, Li L, Yan D, Liang D, Xiao J, Jin H, Wu J, Zhang Y, Chen YH. Novel KCNA5 loss-of-function mutations responsible for atrial fibrillation. *J Hum Genet.* 2009;54:277–283. doi: 10.1038/jhg.2009.26.
20. Hong K, Bjerregaard P, Gussak I, Brugada R. Short QT syndrome and atrial fibrillation caused by mutation in KCNH2. *J Cardiovasc Electrophysiol.* 2005;16:394–396.
21. Priori SG, Napolitano C, Schwartz PJ. Low penetrance in the long-QT syndrome: clinical impact. *Circulation.* 1999;99:529–533.
22. Otagiri T, Kijima K, Osawa M, Ishii K, Makita N, Matoba R, Umetsu K, Hayasaka K. Cardiac ion channel gene mutations in sudden infant death syndrome. *Pediatr Res.* 2008;64:482–487. doi: 10.1203/PDR.0b013e3181841eca.
23. Watanabe H, Darbar D, Kaiser DW, Jiramongkolchai K, Chopra S, Donahue BS, Kannankeril PJ, Roden DM. Mutations in sodium channel beta1- and beta2-subunits associated with atrial fibrillation. *Circ Arrhythm Electrophysiol.* 2009;2:268–275. doi: 10.1161/CIRCEP.108.779181.
24. Sudandiradoss C, Sethumadhavan R. In silico investigations on functional and haplotype tag SNPs associated with congenital long QT syndromes (LQTSs). *Genomic Med.* 2008;2:55–67. doi: 10.1007/s11568-009-9027-3.
25. Yang RQ, Jabbari J, Cheng XS, Jabbari R, Nielsen JB, Risgaard B, Chen X, Sajadieh A, Haunso S, Svendsen JH, Olesen MS, Tfelt-Hansen J. New population-based exome data question the pathogenicity of some genetic variants previously associated with Marfan syndrome. *BMC Genet.* 2014;15:74. doi: 10.1186/1471-2156-15-74.
26. Campbell CM, Campbell JD, Thompson CH, Galimberti ES, Darbar D, Vanoye CG, George AL Jr. Selective targeting of gain-of-function KCNQ1 mutations predisposing to atrial fibrillation. *Circ Arrhythm Electrophysiol.* 2013;6:960–966. doi: 10.1161/CIRCEP.113.000439.
27. Mann SA, Otway R, Guo G,Soka M, Karlsdotter L, Trivedi G, Ohanian M, Zodgekar P, Smith RA, Wouters MA, Subbiah R, Walker B, Kuchar D, Sanders P, Griffiths L, Vandenberg JI, Fatkin D. Epistatic effects of potassium channel variation on cardiac repolarization and atrial fibrillation risk. *J Am Coll Cardiol.* 2012;59:1017–1025. doi: 10.1016/j.jacc.2011.11.039.

Circulation
Arrhythmia and Electrophysiology

American Heart Association®

Functional Characterization of Rare Variants Implicated in Susceptibility to Lone Atrial Fibrillation

Kenshi Hayashi, Tetsuo Konno, Hayato Tada, Satoyuki Tani, Li Liu, Noboru Fujino, Atsushi Nohara, Akihiko Hodatsu, Toyonobu Tsuda, Yoshihiro Tanaka, Masa-aki Kawashiri, Hidekazu Ino, Naomasa Makita and Masakazu Yamagishi

Circ Arrhythm Electrophysiol. 2015;8:1095-1104; originally published online June 30, 2015;
doi: 10.1161/CIRCEP.114.002519
Circulation: Arrhythmia and Electrophysiology is published by the American Heart Association, 7272 Greenville Avenue, Dallas, TX 75231

Print ISSN: 1941-3149. Online ISSN: 1941-3084

PLOS ONE

RESEARCH ARTICLE

Gender Differences in the Inheritance Mode of RYR2 Mutations in Catecholaminergic Polymorphic Ventricular Tachycardia Patients

Seiko Ohno[1,2,3], **Kanae Hasegawa**[1,4], **Minoru Horie**[1]*

1 Cardiovascular and Respiratory Department, Shiga University of Medical Science, Otsu, Japan, **2** Center for Epidemiologic Research in Asia, Shiga University of Medical Science, Otsu, Japan, **3** Department of Cardiovascular Medicine, Kyoto University Graduate School of Medicine, Kyoto, Japan, **4** Department of Cardiovascular Medicine, University of Fukui Faculty of Medical Science, Eiheiji, Japan

* horie@belle.shiga-med.ac.jp

Citation: Ohno S, Hasegawa K, Horie M (2015) Gender Differences in the Inheritance Mode of RYR2 Mutations in Catecholaminergic Polymorphic Ventricular Tachycardia Patients. PLoS ONE 10(6): e0131517. doi:10.1371/journal.pone.0131517

Editor: Tomohiko Ai, Indiana University, UNITED STATES

Received: March 20, 2015

Accepted: June 3, 2015

Published: June 26, 2015

Data Availability Statement: All relevant data are within the paper.

Funding: This study was supported by a grant-in-aid for scientific research from the Japan Society for the Promotion of Science (KAKENHI) (to S.O. 24591575), by a grant for Cardiovascular Diseases from the Ministry of Health, Labour, and Welfare, Japan (to M.H.), by a Research Grant from Takeda Science foundation (to S.O.), by a Research Grant from the Naito foundation (to S.O.), and by a translational Research Grant from the Japanese Circulation Society (to M.H.).

Abstract

Catecholaminergic polymorphic ventricular tachycardia (CPVT) is one of the causes of sudden cardiac death in young people and results from RYR2 mutations in ~60% of CPVT patients. The inheritance of the RYR2 mutations follows an autosomal dominant trait, however, *de novo* mutations are often identified during familial analysis. In 36 symptomatic CPVT probands with RYR2 mutations, we genotyped their parents and confirmed the origin of the respective mutation. In 26 sets of proband and both parents (trio), we identified 17 *de novo*mutations (65.4%), seven from their mothers and only two mutations were inherited from their fathers. Among nine sets of proband and mother, five mutations were inherited from mothers. Four other mutations were of unknown origin. The inheritance of RYR2 mutations was significantly more frequent from mothers (n = 12, 34.3%) than fathers (n = 2, 5.7%) ($P = 0.013$). The mean ages of onset were not significantly different in probands between *de novo* mutations and those from mothers. Thus, half of the RYR2 mutations in our cohort were *de novo*, and most of the remaining mutations were inherited from mothers. These data would be useful for family analysis and risk stratification of the disease.

Introduction

Catecholaminergic polymorphic ventricular tachycardia (CPVT) is an inherited disease characterised by polymorphic ventricular tachycardia induced by exercise or emotional stress in childhood[1]. Sometimes, the first attack of CPVT leads to sudden cardiac death in the young. Five causative genes of CPVT have been reported; RYR2[2], CASQ2[3], KCNJ2[4], TRDN[5] and CALM1[6], and >60% of CPVT patients carry mutations in RYR2[7]. RYR2 gene encodes cardiac ryanodine receptor (RyR2), and RyR2 is indispensable for Ca^{2+} release from sarcoplasmic reticulum (SR), consequently controls the cardiac contraction[8]. CPVT-related RYR2 mutations were reported to cause abnormal calcium leak from SR[9].

Competing Interests: The authors have declared that no competing interests exist.

The inheritance mode of CPVT is both autosomal dominant and recessive; mutations in RYR2[2], KCNJ2[4] and CALM1[6] follow a dominant trait, CASQ2[3] and TRDN[5], recessive. Among RYR2-positive CPVT patients, large CPVT families with RYR2 mutations have been reported in the literature, however, sporadic cases have also been frequently found. We recently demonstrated two families with RYR2 exon 3 deletion[10]. In both families, the mutation was inherited from the maternal side, and there was only one male among six carriers of this exon deletion mutation. As the inheritance mode or frequency of *de novo* RYR2 mutation has not been extensively studied, this study searched for the characteristics of RYR2 mutations in the view of their mode of inheritance.

Methods

Study Cohort

The study cohort consisted of 36 Japanese CPVT probands (18 boys) with RYR2 mutations, their 62 parents and their 29 siblings. All the probands suffered syncope or cardiac pulmonary arrest (CPA) and were registered for genetic screening between 2005 and 2013 in Shiga University of Medical Science. Genetic analysis was performed after obtaining written informed consent in accordance with the study protocol approved by the Institutional Review Board of Shiga University of Medical Science. The approved number is 23–128. In the study protocol, we included the statement that the research results would be published with anonymized clinical information. If the participants were minors or children, we obtained the informed consent verbally from them and written consent from their guardians. The verbal consent was recorded in the clinical record, and our Institutional Review Board approved to obtain written consent from their guardians. According to the participating family members, we divided them into three groups: 26 sets of proband and both parents (trio), 9 sets of proband and mother (P-M) and 1 sets of proband and father (P-F) (Fig 1). All the participating parents were also genotyped, and the origin of the mutation was classified into four groups: *de novo*, from mother, from father and unknown. Their consanguinity of *de novo* group were confirmed by screening of 15 single nucleotide polymorphisms and 1 microsatellite. The unknown group included the case where the inheritance mode could not be determined due to the non-participation of either one of their parents. We evaluated the clinical and genetic characteristics of the probands and compared them in two groups: *de novo* and maternal origin. The mutation locations were classified into three groups based on the previous report [11]. In 23 trio families, we compared the age of parents at the birth of the probands in three groups: *de novo*, maternally- and paternally originated mutations.

Statistical analysis

All continuous variables are reported as mean ± SD. Differences between continuous variables were evaluated using unpaired Student *t*-test or Mann-Whitney Rank Sum Test, and categorical variables were analysed using Fisher exact test. Statistical significance was considered at $P<0.05$.

Results

Origin of the mutations

In 26 mutations identified in 26 probands of the trio group, 17 RYR2 mutations were confirmed to be *de novo*, seven mutations were from their mothers and two from their fathers. (Fig 1 and Table 1). One of the fathers (patient 15) was suspected to carry the mutation in mosaicism (Fig 2). Five mutations from nine mutations in the P-M group were inherited from

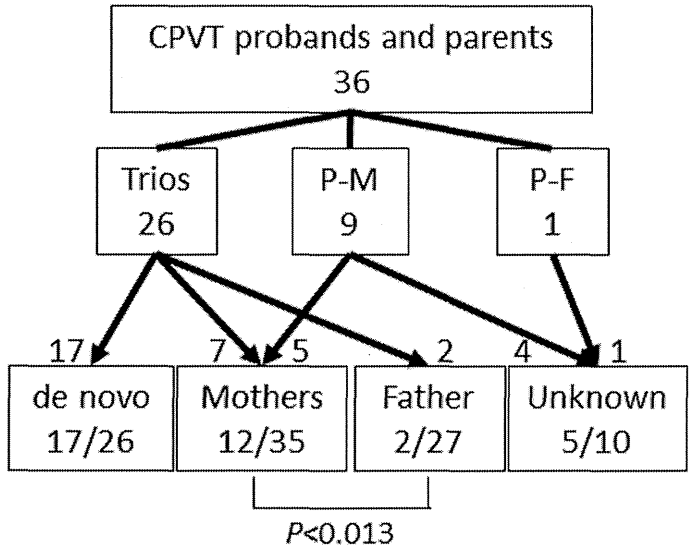

Fig 1. Scheme for Mutation Inheritance. Showing the number of screened family members and the origin of RYR2 mutations. The boxes in the middle lane show genotyped family members in each group. Trio; proband and both parents, P-M; proband and mother, P-F; Proband and father.

doi:10.1371/journal.pone.0131517.g001

their mothers, and four were unknown origin; *de novo* or from their fathers. Although four fathers in the P-M group did not agree to the genetic analysis, they were all healthy and had no history of syncope or cardiac arrest. The mother and maternal grandmother of patient 26 (Table 1) died suddenly at a young age, and his sister carried the same mutation. Accordingly, the mutation appeared to come from his mother side, but we failed to obtain their maternal genomic information. Therefore, his mutation was consequently classified as unknown origin.

In total, 17 mutations were confirmed to be *de novo* from the 26 trio group, 12 were from 35 mothers and only two were from 27 fathers (Fig 1). The frequency of mutations originating from mothers was significantly higher than that from fathers ($P = 0.013$). Five of 12 mothers with mutations suffered syncope and were diagnosed as CPVT after the diagnosis of their children. In contrast, no father had symptoms nor was diagnosed as CPVT (Table 1).

We extended the genetic analysis in the 29 siblings of the probands from 21 families; 14 in *de novo*, 9 in maternal origin, one in paternal origin and 5 in unknown mutation origin. We identified 4 siblings with mutations in maternal origin families and one sibling with a mutation in a paternal origin family, though there were no genotype positive siblings in families of probands with *de novo* mutation. The result suggested the low possibility of germline mosaicism in *de novo* families.

Location of mutations

Among 12 mutations inherited from mothers, seven (58.3%) were located in the N-terminus, while only four (23.6%) from 17 *de novo* mutations were located in the N-terminus (Table 1). Regarding four *de novo* N-terminal mutations, three were at residue 169. In contrast, two maternal mutations (16.7%) were located in the central domain and three (12.5%) were located in the C-terminus. Both paternal mutations were located in the central domain.

Table 1. Clinical and genetic summaries of probands.

		Age			RYR2 mutation					Phenotype of Parents	
Patient Number	Sex	Genetic Analysis	Onset	Most severe symptom	Nucleotide	Amino Acids	Location	Genotyped Family Members	Inheritance	Father	Mother
1	F	17	16	Syncope	exon 3 deletion	N57_G91del35	NT	Trio	Maternal	none	AF
2	F	11	9	Syncope	exon 3 deletion	N57_G91del35	NT	P-M	Maternal	none	syncope
3	F	9	9	Syncope	506g>t	R169L	NT	Trio	de novo	none	none
4	F	5	5	CPA	506g>a	R169Q	NT	Trio	de novo	none	none
5	F	9	9	CPA	506g>a	R169Q	NT	Trio	de novo	none	none
6	M	16	16	CPA	533g>c	G178A	NT	Trio	de novo	none	none
7	M	13	11	Syncope	1221a>t	R407S	NT	P-M	de novo or F	none	none
8	F	12	7	CPA	1259g>a	R420Q	NT	P-M	Maternal	none	syncope
9	M	3	3	Syncope	3667a>g	T1223A	NT	Trio	Maternal	none	none
10	F	11	11	Syncope	3766c>a	P1256T	NT	Trio	Maternal	none	none
11	F	15	12	Syncope	4552c>t	L1518F	NT	Trio	Maternal	none	none
12	F	25	10	Syncope	5170g>a	E1724K	NT	P-M	Maternal	none	syncope
13	M	13	13	CPA	6574a>t	M2192L	Central	Trio	Maternal	none	none
14	M	13	13	CPA	6737c>t	S2246L	Central	Trio	de novo	none	none
15	M	14	14	Syncope	7024g>a	G2342R	Central	Trio	Paternal (mosaic)	none	none
16	M	11	10	CPA	7169c>t	T2390I	Central	Trio	Paternal	none	none
17	M	15	10	CPA	7199g>t	G2400V	Central	Trio	de novo	none	none
18	M	12	12	CPA	7423g>t	V2475F	Central	P-M	de novo or P	none	none
19	F	18	8	CPA	11583g>c	Q3861H	Central	Trio	de novo	none	none
20	F	8	8	Syncope	11583g>t	Q3861H	Central	Trio	de novo	none	none
21	F	27	6	Syncope	11836g>a	G3946S	Central	P-M	de novo or P	none	none
22	F	16	6	Syncope	11836g>a	G3946S	Central	Trio	de novo	none	none
23	F	28	28	CPA	11917g>a	D3973N	Central	Trio	Maternal	none	none
24	M	3	3	Syncope	12006g>a	M4002I	Central	Trio	de novo	none	none
25	M	9	9	Syncope	12371 g>a	S4124N	CT	P-M	Maternal	none	none
26	M	11	11	CPA	12458g>t	S4153I	CT	P-F	de novo or M	none	SD
27	M	11	2	Syncope	12533a>g	N4178S	CT	Trio	de novo	none	none
28	F	6	6	CPA	12579c>g	C4193W	CT	Trio	de novo	none	none
29	M	10	10	Syncope	13463a>c	Q4488P	CT	Trio	de novo	none	none
30	F	33	9	Syncope	13798t>c	F4600L	CT	Trio	de novo	none	none
31	M	28	10	Syncope	14174a>g	Y4725C	CT	Trio	de novo	none	none
32	F	23	9	Syncope	14311g>a	V4771I	CT	P-M	Maternal	none	syncope
33	M	13	13	CPA	14311g>a	V4771I	CT	P-M	de novo or P	none	none
34	M	17	14	CPA	14806c>a	Q4936K	CT	Trio	de novo	none	none
35	M	5	5	CPA	14834_14835insTCA	4944_4945insH	CT	Trio	de novo	none	none
36	M	12	5	CPA	9910c>g, 14222c>t	Q3304E, A4741V	Central and CT	Trio	Maternal	none	syncope

CPA; cardiac pulmonary arrest, NT; N-terminal, CT; C-terminal, SD; sudden death

doi:10.1371/journal.pone.0131517.t001

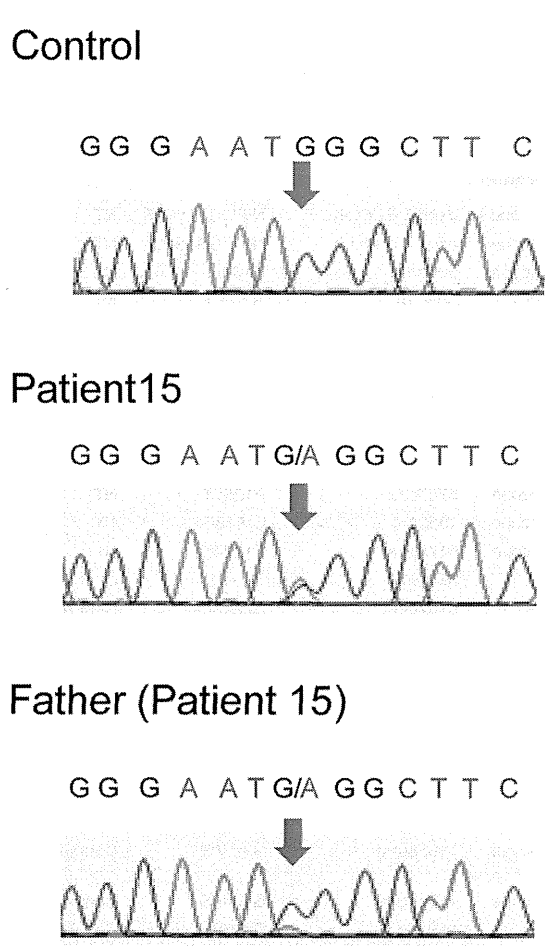

Fig 2. Sequence Electropherograms of Patient 15. Sequence electropherogram of control (upper), patient 15 (middle) and his father (bottom). The peak of the mutant 'a' allele in 7024 residue (red arrow) was lower than the original 'g' peak in the sequence electropherogram of the father, which suggested the presence of mosaicism.

doi:10.1371/journal.pone.0131517.g002

Clinical comparison between de novo and the P-M group

We compared clinical characteristics between 17 probands with *de novo* mutations and 12 with mutations from the maternal side (Table 2). In the *de novo* mutation group, nine probands

Table 2. Clinical characteristics of probands with *de novo* or maternal mutations.

	de novo **n = 17**	**Maternal n = 12**
Male n (%)	9 (52.9)	3 (27.2)
Mean age of Onset	8.4±3.6	11.0±6.4
CPA n (%)	9 (52.9)	4 (33.3)
Syncope n (%)	8 (47.1)	7 (66.7)

doi:10.1371/journal.pone.0131517.t002

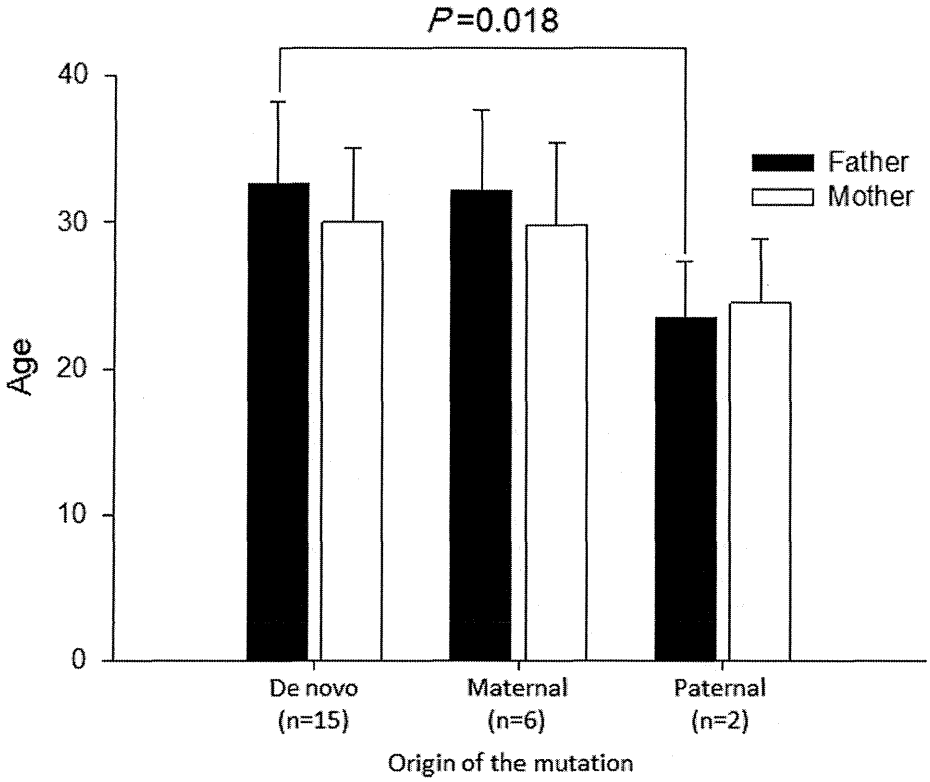

Fig 3. Mean Age of parents depends on the RYR2 mutation origin. Bar graphs depict mean ages of parents at the birth of probands. Filled bars indicate those of fathers and open bars those of mothers. The mean age of genotype-positive fathers was significantly younger than that of the *de novo* mutation group.

doi:10.1371/journal.pone.0131517.g003

(52.9%) were male, while in the maternal mutation group there were only four males (33.3%). The mean ages of onset were younger in *de novo* mutation carriers (8.4 ± 3.6 y.o.) than in mother oriented mutation carriers (11.0 ± 6.4 y.o.). There was no significant difference in the severity of symptoms between the two groups.

Ages of parents at birth of probands

In 23 trio families, we examined the ages of parents at the births of probands (Fig 3). According to the category of RYR2 mutations, there were 15 *de novo*, six maternal and two paternal origin. The mean age of fathers carrying mutations was significantly younger than that in the *de novo* group (23.5 ± 4.9 y.o. vs. 32.6 ± 5.3 y.o. $P = 0.019$). On the other hand, there was no difference of the ages among mothers.

Discussion

In the present study, we first demonstrated that almost half of CPVT-related RYR2 mutations were *de novo*, and the remaining were mostly inherited from mothers. Although the inheritance of CPVT caused by RYR2 mutations follows an autosomal dominant trait, the high

frequency of *de novo* mutations would result in higher occurrence of sporadic cases and thereby confusing the precise diagnosis of CPVT.

One of the most well-known *de novo* mutations is FGFR3-G380R, which is detected in more than 98% of patients with achondroplasia [12]. Advanced paternal age has been shown to increase the risk for the disease, and germline mutation in sperm has been reported in the disease. In RYR2 mutations, we showed that the age of fathers in the *de novo* mutation group was older than that of fathers with mutations, though the number of paternal inheritance was small, and mosaicism may be present in one of the fathers.

Several reports have investigated the inheritance of RYR2 mutations identified in CPVT. Priori et al.,[13] demonstrated that RYR2 mutations were identified in 14 families, and 10 of these 14 mutations were *de novo* and two were inherited from mothers and only one was inherited from the father. The remaining one mutation was probably inherited from the maternal side because she died suddenly at 38 years old. Notably, two genotype-positive mothers in their report were symptomatic, while one genotype-positive father was not. Thus, there was a possibility that the paternal mutation was not the major cause of CPVT, just a rare variant. In our study, two genotype-positive fathers were also asymptomatic, and their mutation sites were very close (residue 2342 and 2390).

In contrast, a dissimilar inheritance pattern was reported in 2012[11]. In familial evaluation with RYR2 mutations, 17 families confirmed the inheritance of RYR2 mutations; six in both *de novo* and maternal, and five in paternal. In the report, we could not obtain the phenotype of their parents or confirm the malignancy of mutations; however, the high paternal mutation inheritance differed from that reported in the previous study.

The low frequency of paternal inheritance may result from the poor prognosis of male patients compared to females[13]. Male CPVT patients might die before the age of reproduction. Indeed, we found that fathers of probands with paternal RYR2 mutations were younger than those of probands with *de novo* mutations. Recently, flecainide therapy for prevention of polymorphic ventricular tachycardia has been prevalent[14, 15], and adequate ICD implantation will improve the prognosis of CPVT patients. These therapies may change the inheritance mode of RYR2 mutations in CPVT in the future.

Study Limitation

Although we reported that half of the RYR2 mutations identified in CPVT were *de novo*, we could not completely rule out cases of mosaicism by PCR-based Sanger methods. In addition, we could not search for the germline mosaicism using other organs nor next generation sequencing analysis to detect low frequency mosaicism.

Conclusions

Almost half of RYR2 mutations identified in CPVT patients were *de novo*, and others were mainly inherited from their mothers. Parents with RYR2 mutations often remain asymptomatic, therefore we need a strict and detailed history taking, exercise tolerance test and genetic survey to prevent a severe cardiac phenotype occurring in younger mutation carriers and their siblings.

Acknowledgments

We are grateful to the families for participating in this study. We thank to Ms. Madoka Tanimoto, Ms. Arisa Ikeda and Ms. Kazu Toyooka for helping us with their expert techniques.

Author Contributions

Conceived and designed the experiments: SO MH. Performed the experiments: SO KH. Analyzed the data: SO. Contributed reagents/materials/analysis tools: SO KH. Wrote the paper: SO MH.

References

1. Hayashi M, Denjoy I, Extramiana F, Maltret A, Buisson NR, Lupoglazoff JM, et al. Incidence and risk factors of arrhythmic events in catecholaminergic polymorphic ventricular tachycardia. Circulation. 2009; 119(18):2426–34. doi: 10.1161/CIRCULATIONAHA.108.829267 PMID: 19398665
2. Priori SG, Napolitano C, Tiso N, Memmi M, Vignati G, Bloise R, et al. Mutations in the cardiac ryanodine receptor gene (hRyR2) underlie catecholaminergic polymorphic ventricular tachycardia. Circulation. 2001; 103(2):196–200. PMID: 11208676
3. Lahat H, Pras E, Olender T, Avidan N, Ben-Asher E, Man O, et al. A missense mutation in a highly conserved region of CASQ2 is associated with autosomal recessive catecholamine-induced polymorphic ventricular tachycardia in Bedouin families from Israel. Am J Hum Genet. 2001; 69(6):1378–84. PMID: 11704930
4. Tester DJ, Arya P, Will M, Haglund CM, Farley AL, Makielski JC, et al. Genotypic heterogeneity and phenotypic mimicry among unrelated patients referred for catecholaminergic polymorphic ventricular tachycardia genetic testing. Heart Rhythm. 2006; 3(7):800–5. PMID: 16818210
5. Roux-Buisson N, Cacheux M, Fourest-Lieuvin A, Fauconnier J, Brocard J, Denjoy I, et al. Absence of triadin, a protein of the calcium release complex, is responsible for cardiac arrhythmia with sudden death in human. Hum Mol Genet. 2012; 21(12):2759–67. doi: 10.1093/hmg/dds104 PMID: 22422768
6. Nyegaard M, Overgaard MT, Sondergaard MT, Vranas M, Behr ER, Hildebrandt LL, et al. Mutations in calmodulin cause ventricular tachycardia and sudden cardiac death. Am J Hum Genet. 2012; 91 (4):703–12. doi: 10.1016/j.ajhg.2012.08.015 PMID: 23040497
7. Kawamura M, Ohno S, Naiki N, Nagaoka I, Dochi K, Wang Q, et al. Genetic Background of Catecholaminergic Polymorphic Ventricular Tachycardia in Japan. Circ J. 2013; 77(7):1705–13. PMID: 23595086
8. Bers DM. Cardiac excitation-contraction coupling. Nature. 2002; 415(6868):198–205. PMID: 11805843
9. George CH, Jundi H, Walters N, Thomas NL, West RR, Lai FA. Arrhythmogenic mutation-linked defects in ryanodine receptor autoregulation reveal a novel mechanism of Ca^{2+} release channel dysfunction. Circ Res. 2006; 98(1):88–97. PMID: 16339485
10. Ohno S, Omura M, Kawamura M, Kimura H, Itoh H, Makiyama T, et al. Exon 3 deletion of RYR2 encoding cardiac ryanodine receptor is associated with left ventricular non-compaction. Europace. 2014; 16 (11):1646–54. doi: 10.1093/europace/eut382 PMID: 24394973
11. van der Werf C, Nederend I, Hofman N, van Geloven N, Ebink C, Frohn-Mulder IM, et al. Familial evaluation in catecholaminergic polymorphic ventricular tachycardia: disease penetrance and expression in cardiac ryanodine receptor mutation-carrying relatives. Circ Arrhythm Electrophysiol. 2012; 5(4):748–56. doi: 10.1161/CIRCEP.112.970517 PMID: 22787013
12. Rousseau F, Bonaventure J, Legeai-Mallet L, Pelet A, Rozet JM, Maroteaux P, et al. Mutations in the gene encoding fibroblast growth factor receptor-3 in achondroplasia. Nature. 1994; 371(6494):252–4. PMID: 8078586
13. Priori SG, Napolitano C, Memmi M, Colombi B, Drago F, Gasparini M, et al. Clinical and molecular characterization of patients with catecholaminergic polymorphic ventricular tachycardia. Circulation. 2002; 106(1):69–74. PMID: 12093772
14. van der Werf C, Kannankeril PJ, Sacher F, Krahn AD, Viskin S, Leenhardt A, et al. Flecainide therapy reduces exercise-induced ventricular arrhythmias in patients with catecholaminergic polymorphic ventricular tachycardia. J Am Coll Cardiol. 2011; 57(22):2244–54. doi: 10.1016/j.jacc.2011.01.026 PMID: 21616285
15. Watanabe H, Chopra N, Laver D, Hwang HS, Davies SS, Roach DE, et al. Flecainide prevents catecholaminergic polymorphic ventricular tachycardia in mice and humans. Nat Med. 2009; 15(4):380–3. doi: 10.1038/nm.1942 PMID: 19330009

European Heart Journal Advance Access published October 1, 2015

European Heart Journal
doi:10.1093/eurheartj/ehv449

BASIC SCIENCE
Myocardial disease

Genetic defects in a His-Purkinje system transcription factor, *IRX3*, cause lethal cardiac arrhythmias

Akiko Koizumi[1†], Tetsuo Sasano[2†*], Wataru Kimura[3], Yoshihiro Miyamoto[4], Takeshi Aiba[4], Taisuke Ishikawa[5], Akihiko Nogami[6], Seiji Fukamizu[7], Harumizu Sakurada[7], Yoshihide Takahashi[8], Hiroaki Nakamura[9], Tomoyuki Ishikura[10], Haruhiko Koseki[10], Takuro Arimura[5], Akinori Kimura[5], Kenzo Hirao[11,12], Mitsuaki Isobe[11], Wataru Shimizu[13,14], Naoyuki Miura[3], and Tetsushi Furukawa[1*]

[1]Department of Bio-Informational Pharmacology, Medical Research Institute, Tokyo Medical and Dental University, Tokyo, Japan; [2]Department of Biofunctional Informatics, Tokyo Medical and Dental University, Tokyo, Japan; [3]Department of Biochemistry, Hamamatsu University School of Medicine, Hamamatsu, Japan; [4]Department of Preventive Cardiology, National Cerebral and Cardiovascular Center, Suita, Japan; [5]Department of Molecular Pathogenesis, Medical Research Institute, Tokyo Medical and Dental University, Tokyo, Japan; [6]Division of Cardiology, Yokohama Rosai Hospital, Yokohama, Japan; [7]Department of Cardiology, Tokyo Metropolitan Hiroo Hospital, Tokyo, Japan; [8]Cardiovascular Center, Yokosuka Kyosai Hospital, Yokohama, Japan; [9]Division of Cardiology, Hiratsuka Kyosai Hospital, Hiratsuka, Japan; [10]Department of Genetics Groups, RIKEN Center for Allergy and Immunology, Yokohama, Japan; [11]Department of Cardiovascular Medicine, Graduate School of Medicine, Tokyo Medical and Dental University, Tokyo, Japan; [12]Heart Rhythm Center, Tokyo Medical and Dental University, Tokyo, Japan; [13]Department of Cardiovascular Medicine, National Cerebral and Cardiovascular Center, Suita, Japan; and [14]Department of Cardiovascular Medicine, Nippon Medical School, Tokyo, Japan

Received 10 April 2015; revised 17 July 2015; accepted 24 August 2015

Aim Ventricular fibrillation (VF), the main cause of sudden cardiac death (SCD), occurs most frequently in the acute phase of myocardial infarction: a certain fraction of VF, however, develops in an apparently healthy heart, referred as idiopathic VF. The contribution of perturbation in the fast conduction system in the ventricle, the His-Purkinje system, for idiopathic VF has been implicated, but the underlying mechanism remains unknown. *Irx3*/*IRX3* encodes a transcription factor specifically expressed in the His-Purkinje system in the heart. Genetic deletion of *Irx3* provides a mouse model of ventricular fast conduction disturbance without anatomical or contraction abnormalities. The aim of this study was to examine the link between perturbed His-Purkinje system and idiopathic VF in *Irx3*-null mice, and to search for *IRX3* genetic defects in idiopathic VF patients in human.

Methods and results Telemetry electrocardiogram recording showed that *Irx3*-deleted mice developed frequent ventricular tachyarrhythmias mostly at night. Ventricular tachyarrhythmias were enhanced by exercise and sympathetic nerve activation. In human, the sequence analysis of *IRX3* exons in 130 probands of idiopathic VF without *SCN5A* mutations revealed two novel *IRX3* mutations, 1262G>C (R421P) and 1453C>A (P485T). Ventricular fibrillation associated with physical activities in both probands with *IRX3* mutations. In HL-1 cells and neonatal mouse ventricular myocytes, IRX3 transfection up-regulated SCN5A and connexin-40 mRNA, which was attenuated by *IRX3* mutations.

Conclusion IRX3 genetic defects and resultant functional perturbation in the His-Purkinje system are novel genetic risk factors of idiopathic VF, and would improve risk stratification and preventive therapy for SCD in otherwise healthy hearts.

Keywords Ventricular fibrillation • Sudden cardiac death • Cardiac conduction system

* Corresponding author. Tel: +81 3 5803 4950, Fax: +81 3 5803 0364, Email: t_furukawa.bip@mri.tmd.ac.jp (T.F.); Tel: +81 3 5803 5365, Fax: +81 3 5803 5365, Email: sasano.bi@tmd.ac.jp (T.S.)

† These authors contributed equally to this work.

Clinical summary

Irx3 homozygous and heterozygous knock out in mouse resulted in ventricular tachyarrhythmias in the setting of high sympathetic tone in otherwise normal hearts. Novel IRX3 mutations were found in patients with idiopathic ventricular fibrillation that occurred related to physical activities. Our finding should be useful for identification of healthy individuals at high risk of sudden death especially during exercise.

Introduction

Sudden cardiac death (SCD) is a leading cause of mortality in Western countries, with an incidence close to one per 1000 individuals per year.[1] Sudden cardiac death results most frequently from ventricular fibrillation (VF) in the setting of coronary artery disease.[2] In 5–10% of cases, however, SCD and VF occur in the absence of identifiable structural heart disease, referred as idiopathic VF.[2] The mechanism underlying idiopathic VF remains largely unknown, except for rare hereditary cases with genetic mutations in cardiac ion channels or their regulators.

In contrast to the atrium of the heart, where the electrical signal propagates from top to bottom, in the ventricles electrical signals propagate upward from apex to base, resulting in coordinated contraction of the heart and efficient cardiac output. To achieve reverse propagation of electrical signals, the ventricle is equipped with a specialized conduction network, the His-Purkinje system. A plethora of clinical information and recent experimental data have indicated that perturbation in the His-Purkinje system is tightly associated with cardiac arrhythmias and SCD[3,4]; however, the mechanistic and genetic link between the His-Purkinje system and VF remain largely unknown.

Irx3 is a member of the Iroquois homebox homeodomain transcription factors. Irx3 is expressed predominantly in the His-Purkinje system in the heart, and its genetic deletion results in perturbation of the His-Purkinje system in apparently normal hearts.[5] Thus, *Irx3*-null ($Irx3^{-/-}$) mouse should provide a good opportunity to study the relationship between the His-Purkinje system and idiopathic VF. Here we examined the arrhythmogenicity in $Irx3^{-/-}$ mice. Since we found that $Irx3^{-/-}$ mice were highly arrhythmogenic, we subsequently set up for a genetic screening of *IRX3* mutations in patients with idiopathic VF. Our data showed that genetic defects in *Irx3*/*IRX3* are linked to arrhythmias in apparently healthy hearts that mostly occur in the settings with elevated sympathetic nervous system activity.

Methods

Detailed methods are described in Supplementary material.

In vivo and *ex vivo* studies in mice

In wild-type (WT), $Irx3^{+/-}$, and $Irx3^{-/-}$ mice, surface electrocardiogram (ECG) was recorded in the lead II. In subgroup of animals, ambulatory ECG monitoring was performed under baseline, during swimming, after administration of isoproterenol, and after surgical creation of myocardial infarction. Ultrasound echocardiography was performed to evaluate left ventricular contractility and dimension in short-axis view at the level of the papillary muscles. *In vivo* electrophysiological study was performed with a custom-made 1 Fr four polar catheter. *Ex vivo* optical mapping was performed on excised hearts under the Langendorff perfusion with a voltage-sensitive dye, di-4-ANEPPS (Sigma-Aldrich).

Patient collection and detection of mutations

We obtained genome DNA from lymphocytes in patients with VF including idiopathic VF, Brugada syndrome, early repolarization syndrome, and short-QT syndrome. Written informed consents were obtained from the patients and were approved by the institutional review boards of each institute.

Genomic DNA was isolated from blood sample, was amplified with PCR, and direct sequencing was performed.

In vitro analysis

In vitro analysis was performed in HL-1, a cell line derived from mouse atrial myocytes, or in neonatal murine ventricular myocytes. Murine Irx3 with or without mutation was subcloned into plasmid vector, pcDNA3.1+ (Life Technologies) or adenoviral vector pAD-CMV-DEST (Life Technology) and was introduced into HL-1 or neonatal murine ventricular myocytes. Quantitative RT-PCR was performed using extracted murine mRNA.

Statistical analyses

All data are shown in terms of mean and SD values. Two-group comparison was analysed by unpaired two-tailed Student's t-test unless described otherwise, and multiple-group comparison was performed by analysis of variance, followed by the Fisher's protected least significant difference test for comparison of each group. Categorical data were compared with the Fisher's exact test. Statistical analyses were performed with Statview (version 5). P value of $<.05$ was considered statistically significant.

Results

Arrhythmogenicity is increased in $Irx3^{-/-}$ mice

The *Irx3*-null ($Irx3^{-/-}$) mouse that we generated (Supplementary material online, *Figure S1A–C*) showed reduced expression of Cx40 and Scn5a (Supplementary material online, *Figures S4–S7*), and ventricular conduction disturbance as previously reported (Supplementary material online, *Figure S2B* and *Table S1*).[5] Gross anatomical analysis found no apparent malformation, and echocardiography showed no difference in ventricular chamber size, ventricular wall thickness, or left ventricular contractile function between WT and $Irx3^{-/-}$ mice (Supplementary material online, *Figure S3* and *Table S2*). Thus, $Irx3^{-/-}$ mice have disturbance exclusively in the conduction of the His-Purkinje system in otherwise normal hearts, providing a suitable model to evaluate the possible link between His-Purkinje system conduction disturbance and arrhythmogenicity in apparently normal hearts.

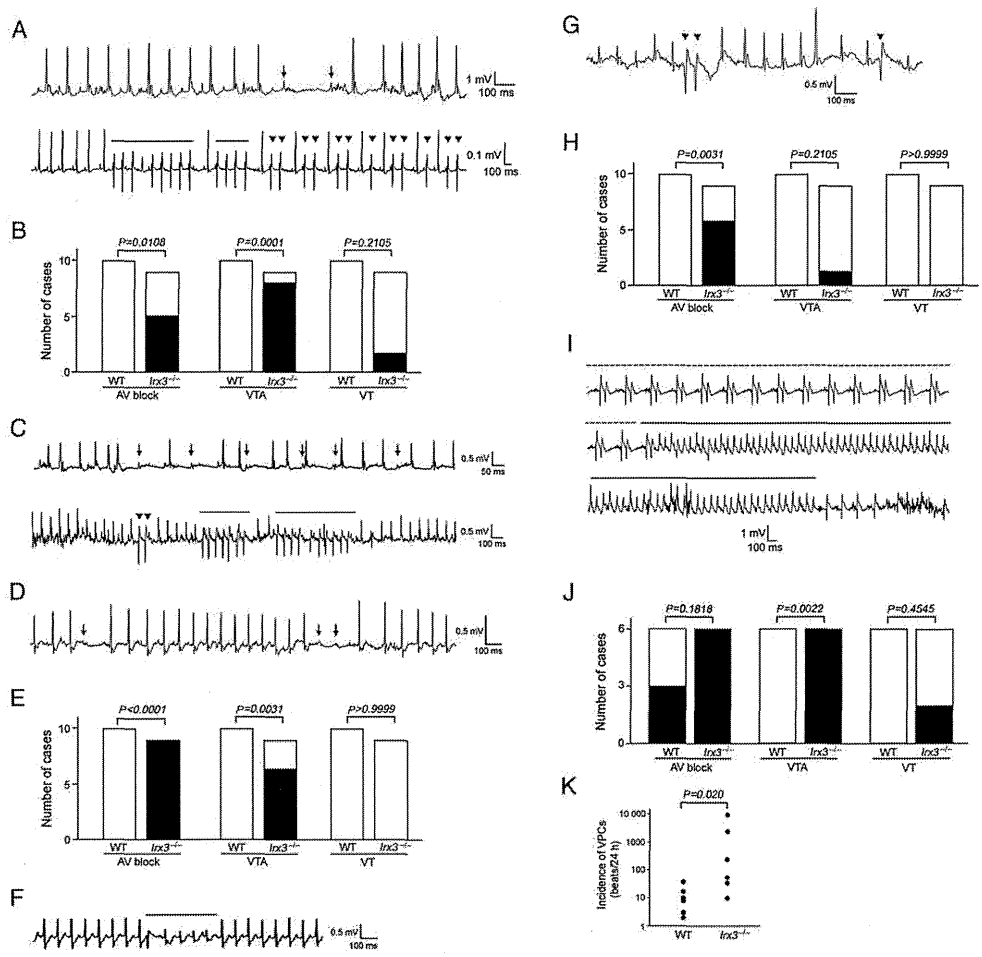

Figure 1 Arrhythmia development in $Irx3^{-/-}$ and $Irx3^{+/-}$ mice. (*A*) Representative ambulatory telemetric electrocardiogram recordings in homozygous $Irx3^{-/-}$ mice. Upper panel shows transient atrio-ventricular block. Arrows indicate P waves without following ventricular excitations. Lower panel shows spontaneous non-sustained ventricular tachycardias. Solid lines indicate the timing with non-sustained ventricular tachycardias. Reverse triangles show ventricular premature contractions. (*B*) Comparison of frequency of atrio-ventricular block, ventricular tachyarrhytmias, and ventricular tachycardias in ambulatory telemetric electrocardiography in WT ($n = 10$) and $Irx3^{-/-}$ ($n = 9$) mice. Ventricular tachyarrhytmias was defined as consecutive ventricular premature contractions more than couplets, and ventricular tachycardias as consecutive ventricular premature contractions more than triplets. Statistical analysis was done with Fisher's exact test. (*C*) Representative ambulatory telemetric electrocardiogram recordings in heterozygous $Irx3^{+/-}$. Upper panel shows transient atrio-ventricular block. Arrows indicate P waves without following ventricular excitations. Lower panel shows spontaneous non-sustained ventricular tachycardias. Solid lines indicate the timing with non-sustained ventricular tachycardias. Reverse triangles show ventricular premature contractions. (*D*) Transient atrio-ventricular block induced by isoproterenol infusion in $Irx3^{-/-}$ mice. Arrows represent P waves without following ventricular excitation. (*E*) Comparison of frequency of atrio-ventricular block, ventricular tachyarrhytmias, and ventricular tachycardias after isoproterenol infusion in WT ($n = 10$) and $Irx3^{-/-}$ ($n = 9$) mice. Statistical analysis was done with by Fisher's exact test. (*F*) Non-sustained ventricular tachycardias induced by isoproterenol infusion in $Irx3^{+/-}$ mice. Solid lines indicate the timing with non-sustained ventricular tachycardias. (*G*) Representative electrocardiogram recordings during swimming in $Irx3^{-/-}$ mice. Reverse triangles show ventricular premature contractions. (*H*) Comparison of frequency of atrio-ventricular block, ventricular tachyarrhytmias, and ventricular tachycardias during swimming in wild-type ($n = 10$) and $Irx3^{-/-}$ ($n = 9$) mice. Statistical analysis was done with Fisher's exact test. (*I*) Representative electrocardiogram recordings within 24 h after surgical creation of myocardial infarction in $Irx3^{-/-}$ mice. Dotted lines indicate the timing with bigeminy, and solid lines indicate the timing with ventricular tachycardias. (*J*) Comparison of frequency of atrio-ventricular block, ventricular tachyarrhytmias, and ventricular tachycardias within 24 h after myocardial infarction in wild-type ($n = 6$) and $Irx3^{-/-}$ ($n = 6$) mice. Statistical analysis was done with Fisher's exact test. (*K*) Incidence of ventricular premature contractions within 24 h after surgical creation of myocardial infarction in wild-type ($n = 6$) and $Irx3^{-/-}$ ($n = 6$) mice. Statistical analysis was done with Mann–Whitney *U* test.

Telemetry ECG recordings in ambulatory conditions showed that both homozygous *Irx3*$^{-/-}$ and heterozygous *Irx3*$^{+/-}$ mice but not WT mice frequently exhibited complete atrio-ventricular (AV) blocks, ventricular tachyarrhytmias (VTAs) defined as consecutive ventricular premature contractions (VPCs) more than couplets, and ventricular tachycardias (VTs) defined as VPCs more than triplets (*Figure 1A–C*). Strikingly, these arrhythmic events occurred predominantly at night, an active phase of mice, implicating relation of these arrhythmias to elevated sympathetic nervous system tone. We tested this possibility by monitoring telemetric ECG under several pathophysiological conditions, in which sympathetic nerve activity is believed to be high. Administration of a sympathetic nerve β-receptor agonist, isoproterenol (0.05 mg/kg, i.p.), induced transient AV block and VTAs in homozygotic *Irx3*$^{-/-}$ mice (*Figure 1D* and *E*) and heterozygotic *Irx3*$^{+/-}$ (*Figure 1F*) mice, but never in WT mice. In *Irx3*$^{-/-}$ mice, ECGs during swimming revealed frequent AV block and occasional VTAs (*Figure 1G* and *H*). In the acute phase of myocardial infarction, activated sympathetic nervous system plays a role in development of life-threatening arrhythmias.[6] Within 24 h after onset of myocardial infarction, *Irx3*$^{-/-}$ mice, but not WT mice exhibited frequent VTAs (*Figure 1I* and *J*). Ventricular premature contractions were seen in both mice: however, the frequency of VPCs was markedly higher in *Irx3*$^{-/-}$ mice than in WT mice (*Figure 1K*).

In the cardiac conduction system, the sino-atrial and AV nodes are innervated by the autonomic nervous systems, while the His-Purkinje system is relatively devoid of autonomic nerve supply. Thus, sympathetic nerve activation enhances the automaticity in the sino-atrial node and the conductivity in the AV node that can stress the His-Purkinje system.[7] We hypothesized that sympathetic nerve activation-induced stress in His-Purkinje system may bring out an arrhythmogenic phenotype. To test this hypothesis, we carried out *ex vivo* optical mapping. In the control condition, propagation of the action potential over the epicardium was significantly slower in *Irx3*$^{-/-}$ mice than in WT mice (1.65 ± 0.50 vs. 1.07 ± 0.32 m/s, $P = 0.047$) (*Figure 2A*), consistent with disturbed conduction in *Irx3*$^{-/-}$ mice in the basal condition. Isoproterenol administration (10 nM) hastened the heart rate both in WT and *Irx3*$^{-/-}$ mice. In all of seven WT mice tested, action potentials exhibited an identical propagation pattern to that of the basal condition—propagation from apex to base—without propagation delay. In four of six *Irx3*$^{-/-}$ mice, action potentials exhibited an entirely different propagation pattern with marked slowing of propagation (*Figure 2B*). In *Irx3*$^{-/-}$ mice, but not in WT mice, various types of arrhythmias including AV block, VTAs, and VTs were detected (*Figure 2C* and *D*).

IRX3 gene defects are found in patients with idiopathic ventricular fibrillation

Next, we asked if genetic defects in *IRX3* are also related to lethal ventricular arrhythmias in human. We analysed the sequence of *IRX3* exons in 130 probands of idiopathic VF, Brugada syndrome, early repolarization syndrome, and short-QT syndrome, in whom mutations in *SCN5A* had not been detected. As a control, the sequence of *IRX3* exons was determined in 250 healthy volunteers.

In the idiopathic VF group, we found two novel mutations of *IRX3* in a family of idiopathic VF with bundle branch block (Family #1, *Figure 3A*) and that without bundle branch block (Family #2, *Figure 3B*), respectively. We examined the sequence of exons in 13 proposed Brugada syndrome-related genes in human (*SCN5A*,

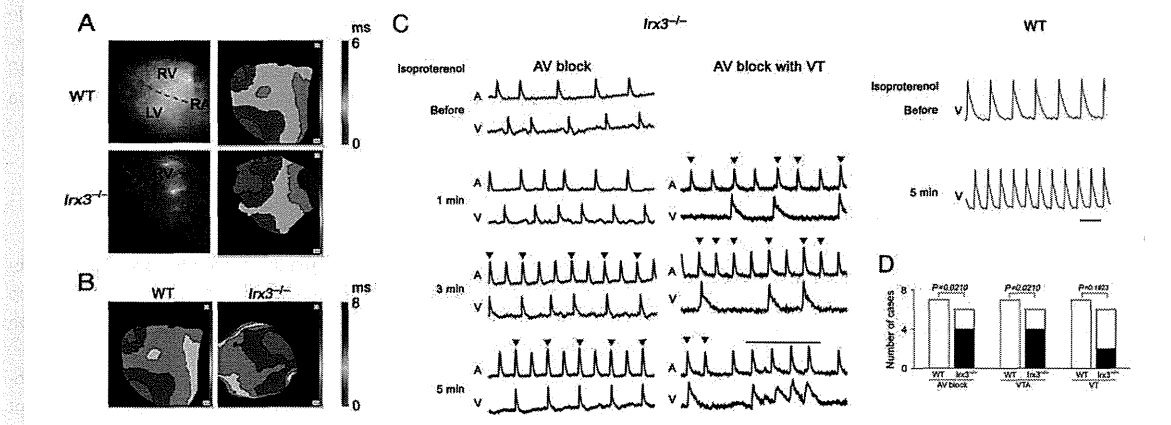

Figure 2 *Ex vivo* optical epicardial mapping and arrhythmia development in *Irx3*$^{-/-}$ mice. (*A*) Representative optical epicardial mapping in wild-type and *Irx3*$^{-/-}$ mice in basal condition. (*B*) Representative optical epicardial mapping in wild-type and *Irx3*$^{-/-}$ mice after isoproterenol application. In *Irx3*$^{-/-}$ mice, epicardial breakthrough occurs from the base of the right ventricle, and propagates to the apex; the propagation of depolarization became markedly slow. (*C*) Arrhythmias observed in wild-type and *Irx3*$^{-/-}$ mice after isoproterenol application. In *Irx3*$^{-/-}$ mice, atrio-ventricular block and atrio-ventricular block with non-sustained ventricular tachycardias occurred. In wild-type mice, only sinus tachycardia occurred. Reverse triangles indicate atrial action potential without following ventricular action potential. Solid bar indicates non-sustained ventricular tachycardias. (*D*) Comparison of frequency of atrio-ventricular block, ventricular tachyarrhytmias, and ventricular tachycardias after isoproterenol injection in wild-type ($n = 7$) and *Irx3*$^{-/-}$ ($n = 6$) mice. Statistical analysis was done with Fisher's exact test.

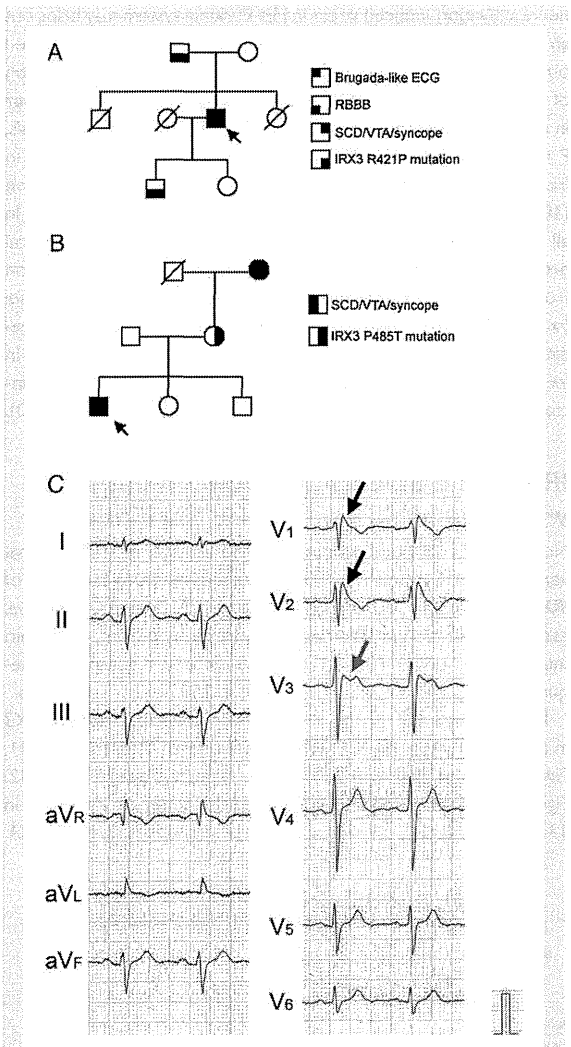

Figure 3 Family pedigrees and surface electrocardiograms in patients without *SCN5A* mutation. (*A*) Pedigree of the Family #1 with R421P IRX3 mutation. An arrow indicates the proband. (*B*) Pedigree of the Family #2 with P485T IRX3 mutation. An arrow indicates the proband. (*C*) Surface electrocardiogram of the proband in the Family #1 with R421P IRX3 mutation. Electrocardiogram showed coved type ST elevation in V1 and V2 (black arrows), and saddle-back type ST elevation in V3 (grey arrow).

GPD1-L, *CACNA1C*, *CACNB2*, *KCNE3*, *SCN1B*, *SCN3B*, *KCNJ8*, *MOG1*, *HCN4*, *KCND3*, *KCNE5*, and *SLMAP*), and found no mutations in any of 130 probands with idiopathic VF or 250 healthy volunteers. The proband in the Family #1 is a 51 y.o. male who developed VF during ice skating. He showed a type 1 Brugada-type ECG with incomplete right bundle branch block (RBBB) pattern (*Figure 3C*). His father had complete AV block demanding pacemaker implantation (Supplementary material online, *Figure S10A*), and his son showed complete RBBB (Supplementary material online, *Figure S10C*). They had an identical point mutation, 1262G>C, resulting in replacement of arginine at residue 421 to proline (R421P) in IRX3. Mother and daughter did not have this mutation, and the ECG was normal (Supplementary material online, *Figure S10B* and *D*). The proband in the Family #2 is a 15 y.o. male and exhibited VF during commuting. His ECG did not show either Brugada-like ECG or early repolarization (Supplementary material online, *Figure S11A*). The proband, grandmother, and mother had identical point mutation, 1453C>A, resulting in replacement of proline at residue 485 to threonine (P485T). The grandmother had experienced syncope with unknown origin, while the mother as well as the father, the sister or the brother did not experience an episode of SCD, VTAs, or syncope. Neither R421P nor P485T mutations were found in 250 healthy volunteers, and were not reported previously including 1000 genomes database.

IRX3 mutations recapitulate Cx40 and Scn5a down-regulation

Since the disturbance of the His-Purkinje system conduction in $Irx3^{-/-}$ mice is attributed to decreased expression of Cx40 and Scn5a, we examined if the *IRX3* mutations found in humans affected the expression of Cx40 and Scn5a. The sequence was highly conserved between human *IRX3* and mouse *Irx3* (85% homologous in nucleotide, and 91% in amino acid) (*Figure 4A*).[8,9] The sites of both mutations were conserved in mouse (reverse triangles in *Figure 4A*). Thus, we infected adenovirus expressing mouse Irx3 without mutation or that with R426P (corresponds to human R421P) or P491T (human P485T) mutation into HL-1 cells, a cell line derived from mouse atrial myocytes or neonatal murine ventricular myocytes. We also performed transfection of Irx3 in pcDNA3 vector into HL-1 cells to exclude the non-specific effect by adenovirus. To exclude the influence of variability in Irx3 expression level, Cx40 and Scn5a mRNA expression was normalized to the expression of Irx3 mRNA using a Ct comparative method. In all three conditions, the transfection of WT Irx3 increased the expression of Cx40 and Scn5a, but not Cx43; up-regulation of Cx40 and Scn5a was significantly less with transfection of each of three mutated Irx3 than with WT Irx3 (*Figure 4B–G*).

Discussion

A certain fraction of SCD occurs in apparently normal hearts, referred as idiopathic VF.[2] We found genetic defects in a transcription factor, *IRX3*, in patients with idiopathic VF. IRX3 is a transcription factor specifically expressed in the His-Purkinje system in the heart[5]; $Irx3^{-/-}$ mouse had disturbance of ventricular fast conduction without anatomical or contraction abnormalities, and exhibited frequent VTAs. Up to the present, genetic defects in at least 13 genes have been linked to idiopathic VF, including Brugada syndrome and early repolarization syndrome. IRX3/Irx3 genetic defects appear to be unique because they predominantly cause disturbance of the His-Purkinje system conduction. The link between genetic defects in cardiac transcription factors and cardiac arrhythmias has previously been reported for Nkx2.5 and Tbx5 in the context of cardiac malformation.[10,11] Among the genetic defects in cardiac transcription factors, the IRX3/Irx3 mutation is also unique because it